AD-A159 916   GEOMETRIC STRUCTURE AND SURFACE VIBRATIONAL RESONANCES: 1/1
              THE BCC FE(111) S..(U) CORNELL UNIV ITHACA NY MATERIALS
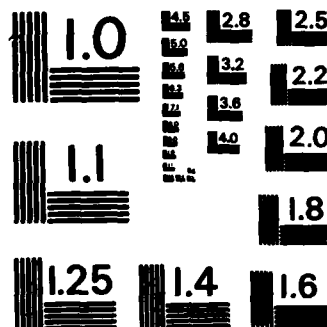   SCIENCE CENTER   J A STROSCIO ET AL. 02 OCT 85 TR-15
UNCLASSIFIED N00014-82-K-0576   F/G 20/12   NL

END

FILMED

DTIC

MICROCOPY RESOLUTION TEST CHART

NATIONAL BUREAU OF STANDARDS-1963-A

OFFICE OF NAVAL RESEARCH

Research Contract No. N00014-K-0576

TECHNICAL REPORT No. 15

GEOMETRIC STRUCTURE AND SURFACE VIBRATIONAL RESONANCES:

THE BCC Fe(111) SURFACE

by

Joseph A. Stroscio, M. Persson, Charles E. Bartosch and W. Ho

Prepared for Publication

in

Physcial Review Letters

Materials Science Center

Cornell University

Ithaca, NY 14853

AD-A159 916

JTIC FILE COPY

DTIC
ELECTE
OCT 0 9 1985
S
E
D

REPORT DOCUMENTATION PAGE		READ INSTRUCTIONS BEFORE COMPLETING FORM
1. REPORT NUMBER 15	2. GOVT ACCESSION NO. AD-A159 916	3. RECIPIENT'S CATALOG NUMBER
4. TITLE (and Subtitle) Geometric Structure and Surface Vibrational Resonances: The BCC Fe(111) Surface		5. TYPE OF REPORT & PERIOD COVERED Interim
		6. PERFORMING ORG. REPORT NUMBER
7. AUTHOR(s) Joseph A. Stroscio, M. Persson, Charles E. Bartosch, W. Ho		8. CONTRACT OR GRANT NUMBER(s) N00014-82-K-0576
9. PERFORMING ORGANIZATION NAME AND ADDRESS Materials Science Center Cornell University Ithaca, NY 14853		10. PROGRAM ELEMENT, PROJECT, TASK AREA & WORK UNIT NUMBERS
11. CONTROLLING OFFICE NAME AND ADDRESS		12. REPORT DATE October 2, 1985
		13. NUMBER OF PAGES 16
14. MONITORING AGENCY NAME & ADDRESS(If different from Controlling Office)		15. SECURITY CLASS. (of this report)
		15a. DECLASSIFICATION/DOWNGRADING SCHEDULE

16. DISTRIBUTION STATEMENT (of this Report)

17. DISTRIBUTION STATEMENT (of the abstract entered in Block 20, If different from Report)

18. SUPPLEMENTARY NOTES

Submitted to Physical Review Letters

19. KEY WORDS (Continue on reverse side if necessary and identify by block number)

20. ABSTRACT (Continue on reverse side if necessary and identify by block number)

The influence of strong multiple interplanar forces is shown to give rise to a new class of surface vibrational resonances on metal surfaces as a result of higher harmonic terms in the bulk phonon dispersion relations. This effect is illustrated with the bcc Fe(111) surface where a surface resonance is observed at 21 meV by high resolution electron energy loss spectroscopy, in excellent agreement with predictions by surface lattice dynamics calculations

GEOMETRIC STRUCTURE AND SURFACE VIBRATIONAL RESONANCES:

THE BCC Fe(111) SURFACE

Joseph A. Stroscio, M. Persson,[†] Charles E. Bartosch, and W. Ho

Laboratory of Atomic and Solid State Physics

and

Materials Science Center

Cornell University

Ithaca, NY 14853

Abstract:

The influence of strong multiple interplanar forces is shown to give rise to a new class of surface vibrational resonances on metal surfaces as a result of higher harmonic terms in the bulk phonon dispersion relations. This effect is illustrated with the bcc Fe(111) surface where a surface resonance is observed at 21 meV by high resolution electron energy loss spectroscopy, in excellent agreement with predictions by surface lattice dynamics calculations.

1985 PACS numbers: 68.30.+z, 63.20.-e, 79.20 kz

Accession For

NTIS GRA&I	☒
DTIC TAB	☐
Unannounced	☐
Justification	

By____

Distribution/

Availability Codes

| Dist | Avail and/or Special |

A-1

MSC Report No. 5650

September 1985

1

With recent advances in the experimental techniques for the study of surface vibrations,[1] considerable interest exists in determining the relation between the geometric structure of the crystal surface and the accompanying surface vibrational modes.[2] Recent electron energy loss measurements have shown the existence of a new type of surface vibrational resonance on the fcc(110) surfaces,[3] which resulted from the unique coordination of the atoms along the fcc(110) direction. This particular coordination along the fcc(110) direction results in a nonmonotonic longitudinal bulk phonon dispersion and a pseudo band gap which give rise to an eigenmode localized at the surface forming a vibrational resonance.

In this paper, we show that this new class[4] of surface vibrational resonances is a general effect which results from higher harmonic terms in the bulk phonon dispersion relation for the longitudinal phonons propagating normal to the surface. These higher harmonic terms allow the existence of a localized solution at the surface-vacuum interface which gives rise to a surface vibrational resonance. We illustrate the generality of this new class of surface resonances with a lattice dynamical analysis of the iron bcc(111) surface where this type of surface resonance is observed by electron energy loss spectrosocpy (EELS). The case considered here corresponds to the $\bar{\Gamma}$ point of the surface Brillouin zone in order to compare to the inelastic dipole scattering observed in the EELS measurements.[6] Our calculations show that these resonances disperse across the surface Brillouin zone and should also be observed at higher parallel wavevector transfers.[7]

The EELS measurements were performed in a multitechnique ultrahigh vacuum system with a base pressure of 4×10^{-11} torr, which is described in detail elsewhere.[8] The EELS spectrometer consists of a double pass 127°

cylindrical deflector for both the monochromator and analyzer. The
electron impact energy was 2.9 eV. The scattering plane containing the
incident and scattered electrons was defined by the crystal normal and the
crystal [0Ī1] direction. The crystal was cleaned extensively in previous
studies.[9] The surface cleaning procedure for the present study included
Neon ion sputtering at 1 keV and annealing to 850 K. Surface cleanliness
was monitored with Auger electron spectroscopy and EELS.

The longitudinal phonon dynamics along high symmetry directions in
cubic crystals reduces to a well-known one-dimensional problem as a result
of the factorization of the dynamical matrix. The one-dimensional dynamics
involves the rigid displacement of lattice planes, where the equations of
motion are given by,[10,11]

$$\omega^2 u_\ell = -\sum_n \frac{\phi_n}{M} (u_{\ell+n} - u_\ell) \tag{1}$$

where u_ℓ is the displacement of an atom in layer ℓ normal to that layer,
M is the mass of the atom, ω is the phonon frequency, and ϕ_n is the force
on a given atom from all the atoms in the neighboring plane n. For the
infinite lattice the equations of motion admit simple plane wave solutions
where the resulting phonon dispersion is given in terms of a Fourier series
in the interplanar force constants ϕ_n as,

$$\omega^2(\zeta) = \sum_n \frac{2\phi_n}{M} (1 - \cos n\pi\zeta), \tag{2}$$

where ζ is the reduced wavevector, $\zeta = Q_z d/\pi$, and d is the interplanar
distance. This relation can then be used to determine the interplanar
force constants from the measured bulk phonon dispersions by inelastic
neutron scattering as has been done extensively in the past.[12]

Surface modes occur in the semi-infinite crystal as a natural consequence of the broken translational symmetry normal to the surface. For the semi-infinite crystal the solutions to the equations of motion in Eq. (1) are no longer simple plane waves but are now modified by the reflection of the phonons at the surface.[3] The surface can be viewed as a perturbation which, given an incident wave on the surface, will mix together reflected waves with the same energy and parallel wavevector. A special situation occurs when the series in Eq. (2) contains terms with $n \geq 2$. For $n \geq 2$ the wavevector corresponding to the reflected phonons becomes complex in certain frequency ranges as determined from the dispersion relations in Eq. (2). These complex wavevectors then gives rise to localized evanescent phonons at the surface. The situation where $n = 2$ was observed on the fcc(110) surface.[3] However, on the bcc(111) surface the interplanar interactions are more extensive and terms at least up to $n = 3$ need to be included in order to describe the lattice dynamics.

The bulk longitudinal phonon dispersion along the Fe(111) direction is shown in Fig. 1, as measured by inelastic neutron scattering.[13] A characteristic feature of the large higher harmonic terms in the phonon dispersion is the appearance of additional maxima and minima within the Brillouin zone as seen in Fig. 1. The occurrence of strong multiple interlayer forces for the bcc(111) direction may be seen from examining the atomic structure along this direction. As Fig. 2 shows, an atom in a layer parallel to the bcc(111) surface has nearest neighboring atoms in the first and third neighboring layers. Next nearest neighboring atoms are located in the second neighboring layer. Thus including only nearest and next nearest neighboring forces, the dispersion along this direction will have up to three harmonic terms in the series expansion in Eq. 2 given

explicitly as,

$$\omega^2(\zeta) = \frac{2}{M} \left\{ \phi_1(1 - \cos\pi\zeta) + \phi_2(1 - \cos2\pi\zeta) + \phi_3(1 - \cos3\pi\zeta) \right\}. \qquad (3)$$

The interlayer force constants may be obtained from a previous general Born-von Karman analysis of the neutron data,[13] and including only the nearest and next nearest interactions they are given by: $\phi_1/M = 96.38$, $\phi_2/M = 68.35$, and $\phi_3/M = 219.14$ meV^2. The dispersion obtained with these force constants is in good agreement with the neutron data as shown by the solid line in Fig. 1. From the bulk dispersion we see that there are three propagating solutions for bulk phonons having energies in the range 23 < $\hbar\omega$ < 35 meV. For energies < 23 meV two of the solutions will exhibit complex wavevectors. For the semi-infinite crystal these complex solutions correspond to evanescent phonons localized at the surface. Since we still have a single propagating solution for this range of frequencies, these evanescent phonons can couple to the overlapping bulk phonons and form a surface resonance. This effect may be seen explicitly by examining the phonon density of states for the semi-infinite crystal projected on the motion of the outer surface layers.

The phonon density of states for the semi-infinite crystal may be evaluated by using an efficient transfer matrix technique.[14] Figure 3 shows the phonon density of states for the longitudinal phonons in Fig. 1 projected on the motion of a bulk layer (upper panel) and the outer surface layer (lower panel). The density of states for the bulk layer shows a region of high density of states for energies >23 meV, with multiple van Hove singularities due to the three stationary points in the phonon dispersion in Fig. 1. For energies < 23 meV the bulk states are severely depleted and hence this region is called a pseudo band gap.[3,7] In this projection the bulk density of states tends to a constant value at

low energies, which is simply proportional to the sound velocity in the dispersion shown in Fig. 1.

The lower panel in Fig. 3 shows the density of states projected on the motion of the outer surface layer. The surface force constants were obtained from considering the loss in coordination obtained from a truncation of the bulk crystal. The interlayer force constants were then simply taken from the bulk values determined above. As seen in this surface projection a very sharp peak is observed within the bulk pseudo band gap at 19.7 meV. Conceptually, the formation of this resonance is similar to the case of true surface phonons which are observed to be split off from the bottom of bulk manifolds into an absolute bulk band gap.[5] In the present case we have a pseudo band gap with a depleted but finite density of bulk states. The surface then splits off a mode from the region of high density of bulk states and becomes resonant with the bulk states in the pseudo band gap. In comparison to the fcc(110) surfaces, the resonance for the bcc(111) surface is significantly stronger and sharper. The intrinsic width for the Fe(111) surface is 0.9 meV compared to 3.5 meV calculated for the Ni(110) surface.[3] This results from the enhanced depletion of bulk states in the pseudo band for the bcc(111) structure in comparison to the fcc(110) structure. The additional small structure at 21.3 meV in the surface density of states is due to a second resonance which is mainly localized on the second and third layers, while the former at 19.7 meV is mainly localized on the first and second layers.

A comparison with the predictions of the surface lattice dynamical calculations can be made with the measured EELS loss spectra shown in Fig. 4. A loss feature attributed to the structural surface resonance is measured at 21 meV. The small structure at ~ 60 meV is due to a small

amount, $\leq 1\%$, of oxygen contamination which does not affect the observation of the surface resonance for very low oxygen coverages. The measured EELS intensity for the dipole active losses is directly proportional to the surface density of states, $g(\omega)$, projected onto a normalized dipole active charge field v^*,[14]

$$g(\omega, \{v^*\}) = \sum_\lambda \left| \sum_\ell v_\ell^* \xi_\ell^{(\lambda)} \right|^2 \delta(\omega - \omega_\lambda),$$ (4)

where $\xi_\ell^{(\lambda)}$ is the normalized displacement of the substrate layer ℓ for an eigenmode λ with energy $\hbar\omega_\lambda$ of the dynamical matrix $\overset{\leftrightarrow}{D}$. For the case of a clean metal surface considered here, the dipole projection is given by the projection on the relative motion of the outer two surface layers.[3,15] The dipole projected density of states is shown in the inset in Fig. 4 for a comparison with the measured loss spectra. The density of states was convoluted with a 4.5 meV Gaussian distribution to simulate the instrumental linewidth. The dipole projection gives a spectral loss peak at 20.6 meV which is in excellent agreement with the measured loss spectra. The slight shift in the dipole projection from the 19.7 meV calculated for the outer surface layer projection is due to the suppression of the asymmetry in the Fano-like shape of the resonance (see Fig. 3) in the dipole projection. In the dipole projection shown in Fig. 4, the density of states goes to zero at low energies, since the two outer surface layers are moving in phase in the long wavelength limit.

In conclusion, we have shown that strong multiple interlayer forces give rise to higher harmonic terms in the bulk phonon dispersion relations which lead to strongly depleted pseudo band gaps and evanescent phonons localized at the surface producing vibrational resonances. This type of resonance is most noticeable in crystal structures which have nearest

neighboring forces in multiple neighboring planes, as is illustrated by the bcc(111) structure.

Acknowledgements

REFERENCES

†Permanent address: Institute of Theoretical Physics, Chalmers

University of Technology, 41296 Göteborg, Sweden.

[1]S. Lehwald, J.M. Szeftel, H. Ibach, T.S. Rahman, and D.L. Mills, Phys. Rev. Lett. 50, 518 (1983). R.B. Doak, U. Harten and J.P. Toennies, Phys. Rev. Lett. 51, 578 (1983).

[2]A recent review of surface vibrations is given by G.I. Stegeman and F. Nizzoli, "Surface Excitations", eds. V.M. Agranovich and R. Loudon, in Modern Problems in Condensed matter Sciences, Vol. 9, (North-Holland, New York, 1984), p. 195.

[3]J.A. Stroscio, M. Persson, S.R. Bare, and W. Ho, Phys. Rev. Lett. 54, 1428 (1985).

[4]Previous lattice dynamical calculations for these surfaces[5] have shown that vibrational resonances can result when a surface mode, which is split off the bottom of a bulk subband, couples to the bulk modes in a second bulk subband. In contrast the resonances discussed in this paper are seen to result from a single bulk phonon band and posses a nonvanishing frequency at the center of the surface Brillouin zone.

[5]R.E. Allen, G.P. Alledredge, and F.W. deWette, Phys. Rev. B 4, 1661 (1971).

[6]Dipole scattering occurs at very small parallel momentum transfers, $Q_\parallel \sim 0$, which corresponds to the center of the surface Brillouin zone. A thorough discussion of the kinematics of dipole scattering in EELS is given by H. Ibach and D.L. Mills, Electron Energy loss Spectroscopy and Surface Vibrations, (Academic, New York, 1982).

[7]M. Persson, J.A. Stroscio, and W. Ho, to be published.

References cont.

[8]J.A. Stroscio, S.R. Bare, and W. Ho, Surf. Sci. 148, 499 (1984).

[9]The Fe(111) crystal was furnished by M. Grunze, University of Maine, Orono, ME.

[10]A.J.E. Foreman and W.M. Lomer, Proc. Phys. Soc. Lond. B 70, 1143 (1957).

[11]C. Kittel, Introduction to Solid State Physics, (Wiley, New York, 1976), p. 107.

[12]J.L. Yarnell, J.L. Warren, and S.H. Koenig, Lattice Dynamics, ed. R.F. Wallis, (Pergamon, New York, 1965), p. 57.

[13]V.J. Minkiewicz, G. Shieane, and R. Nathans, Phys. Rev. 162, 528 (1967).

[14]M. Persson, Phys. Scr. 29, 181 (1984).

[15]S. Andersson, B.N.J. Persson, and N.D. Lang, Phys. Rev. Lett. 52, 2073 (1984).

FIGURE CAPTIONS

Fig. 1. The iron [111] bulk longitudinal phonon dispersion. (■): Measurements by inelastic neutron scattering.[13] (——): The calculated dispersion using the first three interlayer force constants, including only nearest and next nearest neighboring forces, obtained from a previous general Born-von Karman analysis of the neutron data.[13] The force constants are: $\phi_1/M = 96.38$, $\phi_2/M = 68.35$, and $\phi_3/M = 219.14$ meV^2.

Fig. 2. Schematic diagram of the bcc(111) surface structure. (a) Top view. The numbers denote sequential layers of the substrate with number one corresponding to the surface layer. (b) Side view. Notice an atom has nearest neighbors in the first and third neighboring layers. Next nearest neighboring atoms are in the second neighboring layer.

Fig. 3. Vibrational density of states for the longitudinal phonons propagating normal to the surface. The upper panel shows the projection on the motion of a bulk layer. The lower panel shows the projection on the motion of the outer surface layer. Two resonances are observed in the surface density of states at 19.7 and 21.3 meV. The resonance at 19.7 meV is mainly localized on the first and second layers, while the latter at 21.3 meV is mainly localized on the second and third layers.

Fig. 4. An electron energy loss spectra of the Fe(111) surface. The spectrum was recorded at 300 K in the specular direction. The surface resonance is observed in the loss spectrum at 21 meV. The small structure at ~ 60 meV is due to a small amount, < 1%, of oxygen contamination. The inset shows the dipole projected

Figure Captions cont.

density of states for a comparison with the measured loss
spectra. The projection is taken on the relative motion of the
outer two surface layers and is convoluted with a 4.5 meV Gaussian
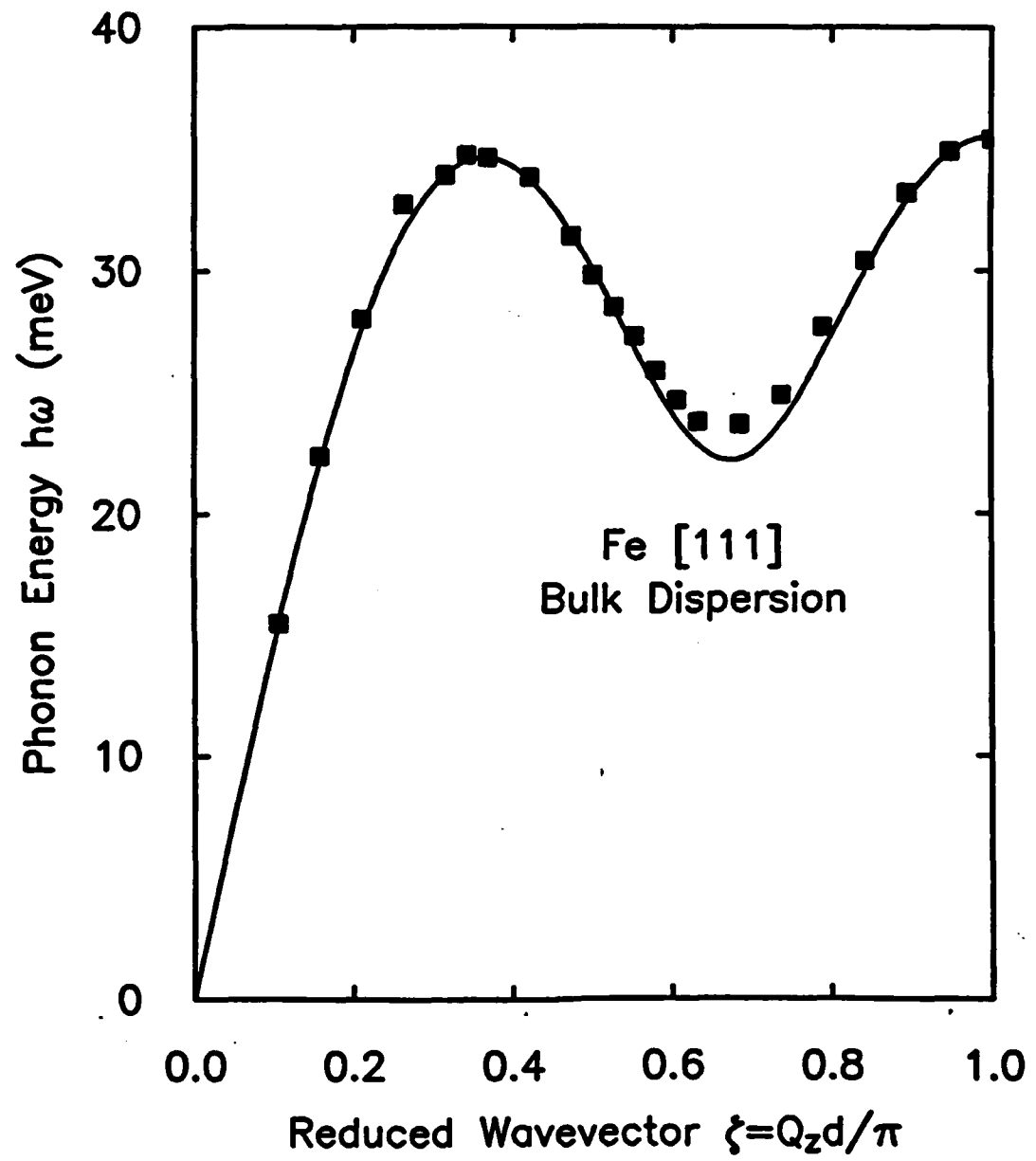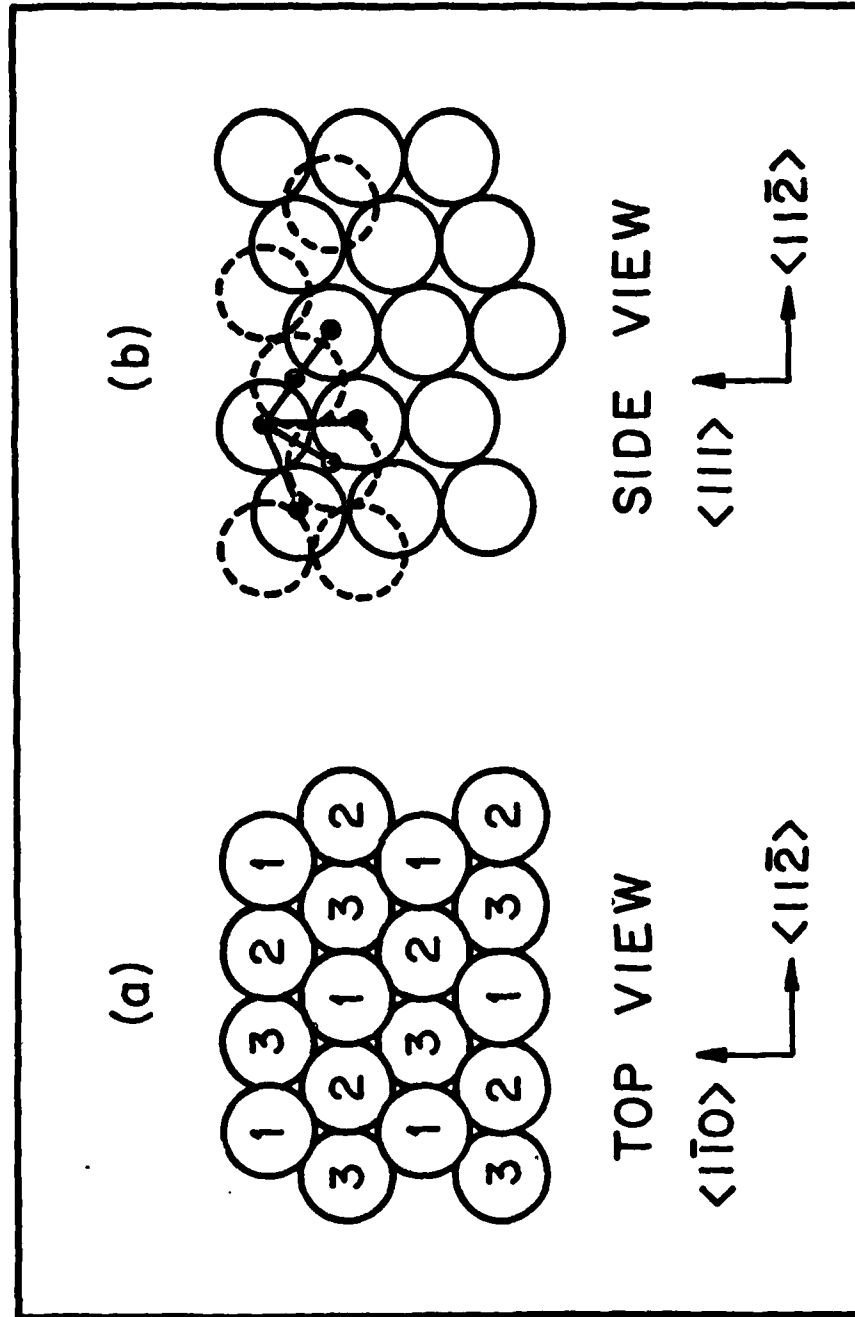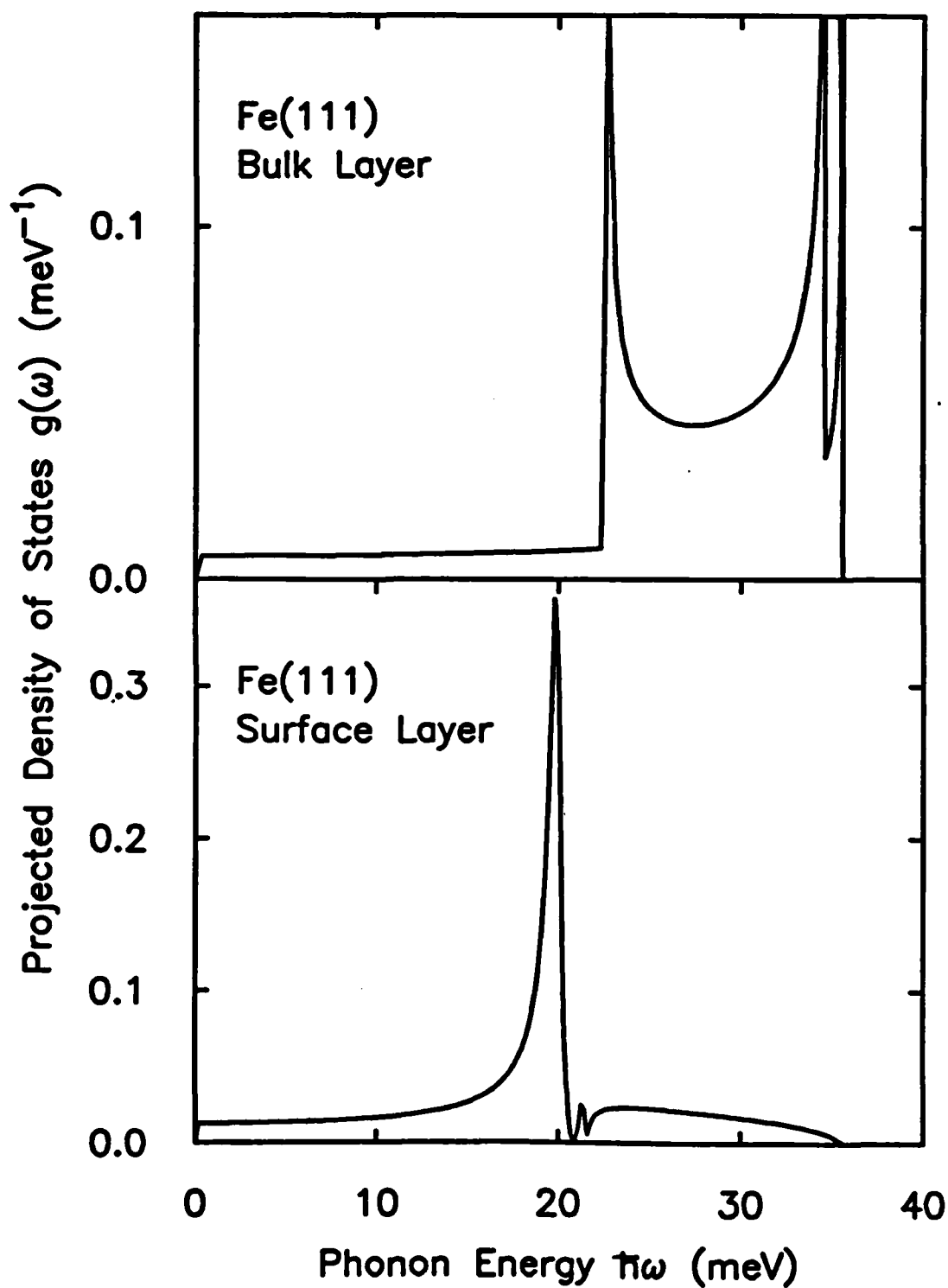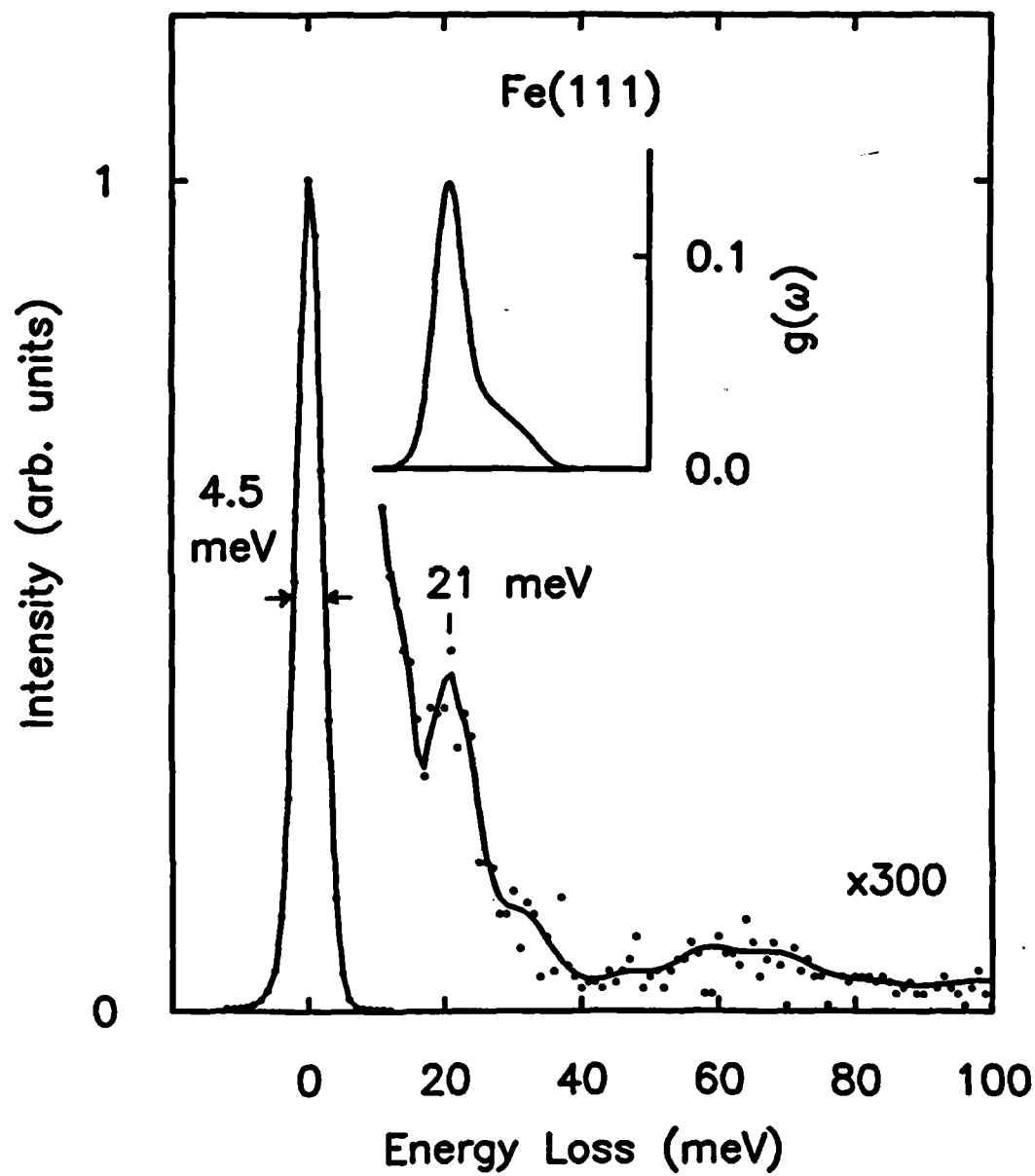distribution to account for the instrumental resolution.

Fig. 1

Fig. 2

Fig. 3

Fig. 4

END

FILMED

11-85

DTIC